Physical Properties of Polyamide 6/Metallocene Isotactic Polypropylene Conjugated Filaments

Kai-Jen Hsiao, Zhi-Feng Jue, Dan-Cheng Kong, Frank L Chen

Fiber Technology Division, Material and Chemical Research Laboratories/Industrial Technology Research Institute, Hsinchu 30055, Taiwan, Republic of China

Received 22 September 2005; accepted 5 January 2006
DOI 10.1002/app.24214
Published online 4 May 2006 in Wiley InterScience (www.interscience.wiley.com).

ABSTRACT: Polyamide 6 (PA 6) and metallocene isotactic polypropylene (m-iPP) polymers were extruded (in proportions of 75/25, 50/50, and 25/75) from two melt twin-screw extruders to prepare three PA 6/m-iPP conjugated filaments. This study investigated the physical properties of PA 6/m-iPP conjugated filaments with gel permeation chromatography, differential scanning calorimetry, thermogravimetric analysis, potentiometry, rheometry, density-gradient measurements, wide-angle X-ray diffraction, extension stress–strain measurements, and scanning electron microscopy. The flow behavior of PA 6/m-iPP polyblended polymers exhibited negative-deviation blends, and a 50/50 PA 6/m-iPP blend showed the minimum value of the melt viscosity. The experimental results from differential scanning calorimetry indicated that PA 6 and m-iPP molecules formed an immiscible system. The tenacity of the PA 6/m-iPP conjugated filaments decreased initially and then increased as the m-iPP content increased. The crystallinities and densities of the PA 6/m-iPP conjugated filaments had a linear relationship with the blend ratio. Morphological observations revealed that the blends had a dispersed-phase structure. A pore/fiber morphology of a larger size (from 0.5 to 3 μm in diameter) was observed after a formic acid (PA 6 was moved)/xylene (m-iPP was moved) treatment on the cross section of a PA 6/m-iPP conjugated filament. PA 6 and m-iPP polymers were proved to be an incompatible system.
 J Appl Polym Sci 101: 1471–1476, 2006

Key words: isotactic; morphology; polyamides; poly(propylene) (PP)

INTRODUCTION

The applications of polyblends are important developments of the plastic and synthetic fiber industries. Polyblends are mixtures of two or more polymers that can either mix completely on a molecular scale or form a two-phase structure. Polyblends can exhibit new combinations of properties that depend on the properties of the components and strongly upon the morphology of the blended materials. The morphology resulting from a blending process depends mainly on the rheological and interfacial properties of the molten components, the blending conditions, and the weight ratio of the blended polymers.[1–3] Polyblends can be characterized by their phase behavior as either miscible or immiscible. The thermal, mechanical, and rheological properties of a polyblend depend strongly on its state of miscibility.[4]

There are some reports on the physical properties of polyamide 6 (PA 6) with other polymers such as poly(ethylene terephthalate), cationic dyeable poly(ethylene terephthalate), poly(butylene terephthalate), cationic dyeable polyamide 6, polyethylene, and Ziegler–Natta isotactic polypropylene.[5–15] Polypropylene resins have been produced from Ziegler–Natta catalysts for over 45 years now. These polymers are typically high-molecular-weight and broad molecular weight distribution (MWD) resins produced in a polymerization reactor. In recent years, these resins have frequently been given a postreactor treatment to narrow their MWDs and lower their molecular weights when they are to be used for fiber spinning. This treatment typically consists of extrusion in the presence of a peroxide compound, which produces the desired result by thermal oxidative degradation of the reactor resin. This method is known as the controlled rheology process. A major advantage of the use of metallocene catalysts for preparing polypropylene is that narrow-MWD resins can be obtained directly from the reactor without the need for secondary processing.[16]

In this study, metallocene isotactic polypropylene (m-iPP) was chosen as a blended material. The PA 6 polymer possesses amide-functional groups (—NHCO— groups). Furthermore, the m-iPP polymer does not possess any functional groups. The interfacial adhesion plays a critical role for PA 6/m-iPP conjugated filaments. This study thoroughly investigated the flow behavior, thermal behavior, crystallinity, mechanical properties, density, and morphology of PA 6/m-iPP conjugated filaments on the island–sea type.

EXPERIMENTAL

Materials and conjugated spinning

PA 6 chips were purchased from Rhodia Engineering Plastics Co., Ltd. (Taipei, Taiwan). The PA 6 resin was

Correspondence to: K.-J. Hsiao (kjhsiao@itri.org.tw).

TABLE I
Characteristics of the PA 6 and m-iPP Chips

Chip	RV[a]	MFR (g/10 min)[b]	M_w (g/mol)	M_w/M_n[c]	R—NH_2 (mequiv/kg)	R—COOH (mequiv/kg)	T_m (°C)	T_d (°C)[d]
PA 6	2.52	—	32,000	1.83	51	64	220.6	328
m-iPP	—	24	175,000	1.92	0	0	150.2	372

[a] Obtained with a 1.0 g/100 mL solution in 96% H_2SO_4 at 25°C.
[b] Measured with the ASTM D 1238 method (230°C/2.16 kg).
[c] Measured for PA 6 and m-iPP in the HFIP and TCB solvent systems, respectively.
[d] Degradation temperature.

a semidull, fiber-grade, crystallized chip with a normal relative viscosity (RV) of 2.52 (at 96% H_2SO_4, 1.0 g/100 mL, and 25°C) and 0.3% TiO_2. Before spinning, PA 6 was dried for 24 h at 105°C. m-iPP chips were obtained from Exxon Mobil Chemical Co. (Houston, TX). The m-iPP resin (Achieve 3854), a white pellet, with an average diameter size of 3–5 mm, was specially designed for the fiber-spinning process. Its nominal melt flow rate (MFR) was 24 g/10 min at 230°C. Table I lists the synthetic characteristics of the PA 6 and m-iPP polymers. The PA 6 and m-iPP polymers were extruded in the proportions of 75/25, 50/50, and 25/75 from two melt twin-screw extruders to prepare three PA 6/m-iPP conjugated filaments.

All conjugated filaments were prepared on an AW-909 bicomponent precision conjugated filament winding machine, which consisted of two 1-in. extruders, two metering pumps, a bicomponent spin pack purchased from Teijin Seiki Co. (Tokyo, Japan), a 15-foot stack with a cross air-cooling channel, a spin finish applicator, and a speed winder. The extrusion temperature of the PA 6 and m-iPP polymers was 260°C. The cross sections of the PA 6/m-iPP conjugated filaments were prepared as an island–sea type, and the combined melts were extruded through 24 round holes 0.2 mm in diameter (32 islands/hole) at 260°C. Three different mass flow rate combinations of PA 6 and m-iPP were used. The extruded conjugated filaments were quenched and subsequently wound to yield the conjugated partially oriented yarn (POY) filaments. Also, single-component PA 6 POY and m-iPP POY were produced. The take-up speed of the winder for all POY filaments was 2800 m/min. Then, POY filaments were drawn 1.61 times to form fully oriented yarn (FOY) filaments by a drawn-winder machine. The draw temperature and take-up speed were 110°C and 300 m/min, respectively. The specification of the FOY filaments was 75d/24f × 32 islands. A Cambridge Steroscan 600 scanning electron microscope (London, UK) was used to examine the morphological structure of each sample, which was sputter-coated with Au to prevent oxidation. Table II shows the compositions of the PA 6/m-iPP conjugated filaments.

Measurements

Gel permeation chromatography (GPC) data were measured with a Waters model 510 (Milford, MA). Two solvent systems were used for the GPC measurement. The MWDs of the PA 6 and m-iPP polymers were measured in 1,1,1,3,3,3-hexafluoro-2-propanol (HFIP) and trichlorobenzene (TCB) solvent systems, respectively. RV of PA 6 was obtained with a 1.0 g/100 mL solution in 96% H_2SO_4 at 25°C.[17] Wide-angle X-ray diffraction (WAXD) studies of the samples were conducted with a MAC Science X-ray unit (Tokyo, Japan) operated at 35 kV and 20 mA. X-ray diffraction was then used with Cu Kα radiation and scanning from 5 to 40° (2θ) with a scan speed of 4°/min.[18–20] Thermogravimetric analysis (TGA) and differential scanning calorimetry (DSC) measurements of the samples were made with a PerkinElmer Pyrix-1 (Boston, MA). The heating rate of the TGA measurements was 10°C/min (from 30 to 600°C). Both the heating rate and cooling rate were 10°C/min (from −30 to 300°C), and the temperature was held for 3 min at 300°C for the DSC measurements. The crystallinity of the DSC method was calculated with the following equation: Crystallinity (%) = $\Delta H_m/\Delta H_m^0 \times 100\%$, where ΔH_m and ΔH_m^0 are the heats of fusion (J/g) of the repeating unit for the sample and 100% crystallinity, respectively. ΔH_m^0 of pure PA 6 (and pure polypropylene) is equal to 230.1 J/g (and 209.0 J/g).[21,22] The densities of the samples were determined with the density-gradient method. A mixture of *n*-heptane and carbon tetrachloride was used for this purpose. The densities of *n*-heptane and carbon tetrachloride solvents were 0.684 and 1.595 g/cm^3, respec-

TABLE II
Compositions of the PA 6/m-iPP Conjugated Filaments

Polymer code	PA 6/m-iPP blend ratio
Sample 1	100/0
Sample 2	75/25
Sample 3	50/50
Sample 4	25/75
Sample 5	0/100

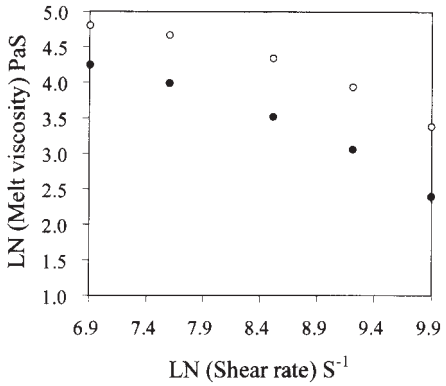

Figure 1 Relationship between the melt viscosity and shear rate for PA 6 and m-iPP polymers at 260°C: (○) PA 6 and (●) m-iPP.

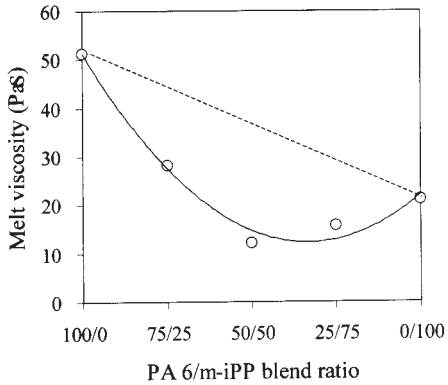

Figure 3 Relationship between the melt viscosity and blend ratio for PA 6/m-iPP polyblended polymers at 260°C/10,000 S^{-1}: (- - -) calculated values and (○) experimental values.

tively. The scale of the density-gradient method was prepared from 0.850 to 1.200 g/cm^3. The melt viscosities of the samples were measured with a capillary rheometer, and the length-to-diameter ratio of the capillary was 30. Scanning electron microscopy (SEM) pictures were taken with a JEOL 200CX (Tokyo, Japan). All stress–strain data for the samples were obtained on a Zwick 1511 Instron instrument (Zwick, Bambery, Germany) at an extension rate of 200 mm/min.

RESULTS AND DISCUSSION

Flow behavior of the polyblended polymers

Figures 1 and 2 present capillary rheological data at temperatures and shear rates applicable to the spinning process. Figure 1 shows the melt viscosities of the PA 6 and m-iPP polymers at 260°C versus the shear rate. From 1000 to 20,000 S^{-1}, the two polymers exhibited pseudoplastic flow behavior. The rheological curves indicated that the melt viscosity of the PA 6 polymer was higher than that of the m-iPP polymer over the entire shear rate range. Figure 2 displays the melt viscosities of the PA 6/m-iPP polyblended polymers at 260°C versus the shear rate. The melt viscosities of the PA 6/m-iPP polyblended polymers also exhibited pseudoplastic flow behavior. This tendency was independent of the blend ratio. Figure 3 shows that the melt viscosities of the PA 6/m-iPP polyblended polymers exhibited negative-deviation blends (NDBs).[23–27] Notably, the 50/50 PA 6/m-iPP blend showed a lower value of the melt viscosity than that predicted by the additivity rule at 260°C and 10,000 S^{-1}. The rheological results indicated poor interfacial adhesion between the PA 6 and m-iPP polymers. The melt viscosities of PA 6, m-iPP, and their blends followed the order PA 6 > 75/25 PA 6/m-iPP > m-iPP > 25/75 PA 6/m-iPP > 50/50 PA 6/m-iPP.

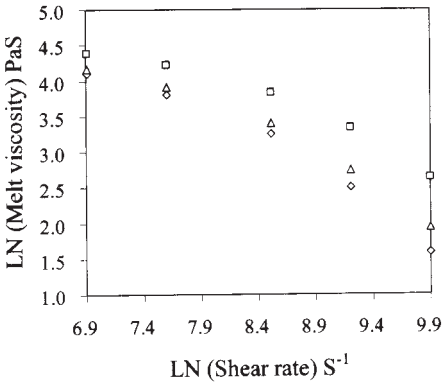

Figure 2 Relationship between the melt viscosity and shear rate for PA 6/m-iPP polyblended polymers at 260°C: (□) 75/25 PA 6/m-iPP, (◇) 50/50 PA 6/m-iPP, and (△) 25/75 PA 6/m-iPP.

Thermal behavior and crystallinity of the conjugated filaments

Table III displays the thermal properties of PA 6, m-iPP, and three PA 6/m-iPP conjugated filaments. In the DSC heating process, the endothermic peaks of the PA 6 and m-iPP filaments occurred at 221.7 and 151.6°C, respectively. The endothermic peak [i.e., the melting temperature (T_m)] was due to the melting of the sample. T_m of the PA 6 and m-iPP filaments was compared with that of the PA 6 and m-iPP chips, as shown in Tables I and III. Because of the influences of the orientation and crystallization, T_m of the PA 6 and m-iPP filaments was clearly higher than that of the PA 6 and m-iPP chips. T_m of the PA 6 filament was higher than that of m-iPP (ca. 70°C). Usually, T_m of PA 6 and m-iPP filaments is noted to be 215–222 and 147–152°C, respectively.[28,29] These DSC curves displayed only a melting endothermic peak, indicating that the PA 6 and m-iPP filaments were originally crystalline. The endothermic peak of 221.7°C corresponded to the α

TABLE III
Thermal Properties of the PA 6, m-iPP, and PA 6/m-iPP Conjugated Filaments

	Heating process				Cooling process					
	PA 6		m-iPP		PA 6			m-iPP		
Polymer code	T_{m1} (°C)	ΔH_{m1} (J/g)	T_{m2} (°C)	ΔH_{m2} (J/g)	T_{cc1} (°C)	ΔH_{cc1} (J/g)	Half-time (s)	T_{cc2} (°C)	ΔH_{cc2} (J/g)	Half-time (s)
Sample 1	221.7	70.1	—	—	184.8	62.7	68.9	—	—	—
Sample 2	219.7	52.6	153.8	24.4	182.9	47.0	—	105.1	24.9	—
Sample 3	218.6	35.1	153.1	48.8	180.5	31.4	—	104.3	49.8	—
Sample 4	218.3	17.5	152.6	73.2	179.8	15.7	—	102.9	74.7	—
Sample 5	—	—	151.6	97.6	—	—	—	102.6	99.6	46.4

phase of the PA 6 filament.[30] On the other hand, the endothermic peak of 151.6°C corresponded to the α phase for the m-iPP filament.[31,32] The α phase of the PA 6 filament was different from that of the m-iPP filament in the physical sense. In the DSC cooling process, the exothermic peaks [i.e., the cold-crystallization temperatures (T_{cc}'s)] of the PA 6 and m-iPP filaments occurred at 184.8 and 102.6°C, respectively. The exothermic peak was due to the recrystallization behavior of the melting polymer. Clearly, the half-time of the recrystallization for the m-iPP filament was shorter than that of the PA 6 filament, and this implied that the recrystallization rate of the m-iPP filament was faster than that of the PA 6 filament. For all the PA 6/m-iPP conjugated filaments, T_m of the PA 6 segments (T_{m1}) nearly did not shift and appeared around 218–220°C. Additionally, T_m of the m-iPP molecules (T_{m2}) also did not clearly change and appeared at 152–154°C. In other words, the T_m change was independent of the blend ratio.

Figure 4 displays the linear variations of ΔH_m with the blend ratio of the PA 6/m-iPP conjugated filaments. ΔH_m of the PA 6 molecules (ΔH_{m1}) proportionally declined with increasing m-iPP content. Meanwhile, ΔH_m of the m-iPP molecules (ΔH_{m2}) proportionally increased with increasing m-iPP content. For all the PA 6/m-iPP conjugated filaments, the T_{cc} point of the PA 6 molecules (T_{cc1}) also nearly did not change and appeared around 180–183°C. The T_{cc} point of the m-iPP molecules (T_{cc2}) was observed around 103–105°C. Figure 5 also shows the linear variations of the recrystallization heat of the exothermic peak (ΔH_{cc}) with the blend ratios of the PA 6/m-iPP conjugated filaments. ΔH_{cc} of the PA 6 molecules (ΔH_{cc1}) proportionally decreased with increasing m-iPP content. Meanwhile, ΔH_{cc} of the m-iPP molecules (ΔH_{cc2}) proportionally increased with increasing m-iPP content. The DSC experimental results indicated that PA 6 segments and m-iPP molecules were an immiscible system.

The heat of fusion was used to indicate the crystalline fraction of the material. A higher heat of fusion was expected to result in a higher crystallinity. Table IV reveals the crystallinities of the PA 6, m-iPP, and PA 6/m-iPP conjugated filaments. The heat of fusion

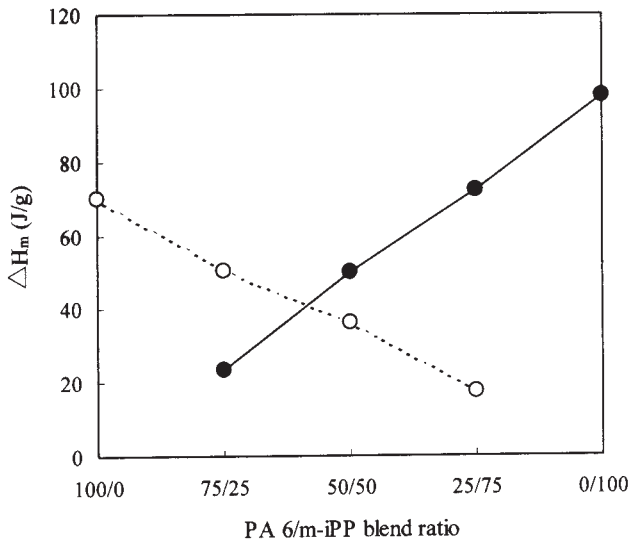

Figure 4 Relationship between ΔH_m and the blend ratio of PA 6/m-iPP conjugated filaments: (○) PA 6 and (●) m-iPP.

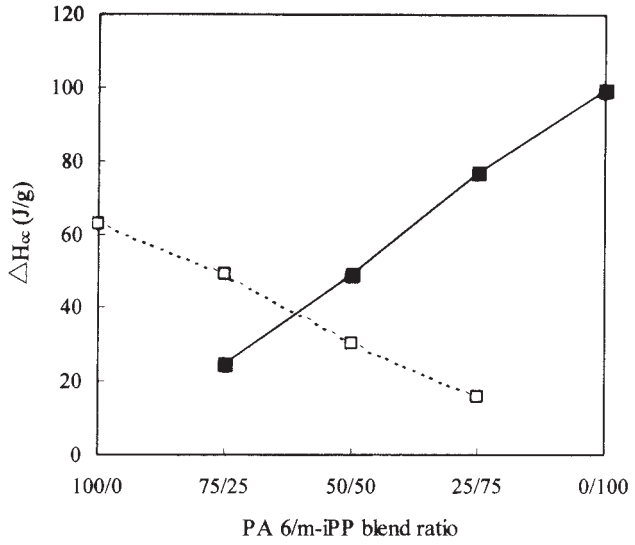

Figure 5 Relationship between ΔH_{cc} and the blend ratio of PA 6/m-iPP conjugated filaments: (□) PA 6 and (■) m-iPP.

TABLE IV
Crystallinity (X_c) Values of the PA 6, m-iPP, and PA 6/m-iPP Conjugated Filaments

	DSC					
	PA 6 part		m-iPP part			
Polymer code	ΔH_{m1} (J/g)	X_c (%)	ΔH_{m2} (J/g)	X_c (%)	Total X_c (%) the of filament	Total X_c (%) of the filament by WAXD
Sample 1	70.1	30.5	—	—	30.5	29.2
Sample 2	52.6	22.8	24.4	11.7	34.5	32.8
Sample 3	35.1	15.2	48.8	23.3	38.6	36.9
Sample 4	17.5	7.6	73.2	35.0	42.6	41.2
Sample 5	—	—	97.6	46.7	46.7	45.3

of melting was used to calculate the crystallinity. Values of 230.1 and 209.0 J/g, corresponding to 100% crystallinity, were used for PA 6 and polypropylene, respectively. The crystallinities of the PA 6 and m-iPP filaments were 30.5 and 46.7%, respectively. The crystallinity of the m-iPP filament was 16.2% higher than that of the PA 6 filament. After blending, the total crystallinity of the PA 6/m-iPP conjugated filament increased as the proportion of m-iPP increased. The crystallinities from the WAXD method were slightly lower than those from the DSC method. Figure 6 displays the relationship between the crystallinities and the blend ratios of the PA 6/m-iPP conjugated filaments. For all the PA 6/m-iPP conjugated filaments, the experimental crystallinities agreed fairly well with the calculated values. This indicated that PA 6 and m-iPP formed an immiscible system.

Morphologies of the conjugated filaments

The morphological observations revealed that the blends had a dispersed-phase structure. As shown in Figure 7(a,b), both the PA 6 and m-iPP filaments had a uniform surface structure on their cross section. As shown in Figure 7(c,d), a pore/fiber morphology of a larger size (from 0.5 to 3 μm in diameter) was observed after a formic acid (PA 6 was moved)/xylene (m-iPP was moved) treatment of the cross section of the 50/50 PA 6/m-iPP conjugated filament. The morphological results could imply that PA 6 and m-iPP could be divided into two parts. Meanwhile, the PA 6 and m-iPP polymers were proved to be an immiscible system.

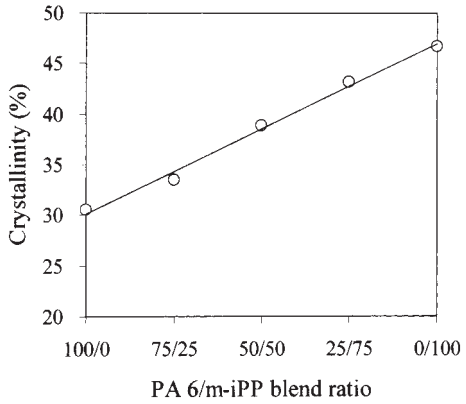

Figure 6 Relationship between the crystallinity and blend ratio of PA 6/m-iPP conjugated filaments.

Mechanical properties and density measurements of the conjugated filaments

Figure 8 shows the relationship between the tenacities and blend ratios of the PA 6/m-iPP conjugated filaments. The tenacities of the PA 6/m-iPP conjugated filaments declined initially and then increased with a proportion of m-iPP. Obviously, the 50/50 PA 6/m-iPP blend displayed a minimum value. The poor in-

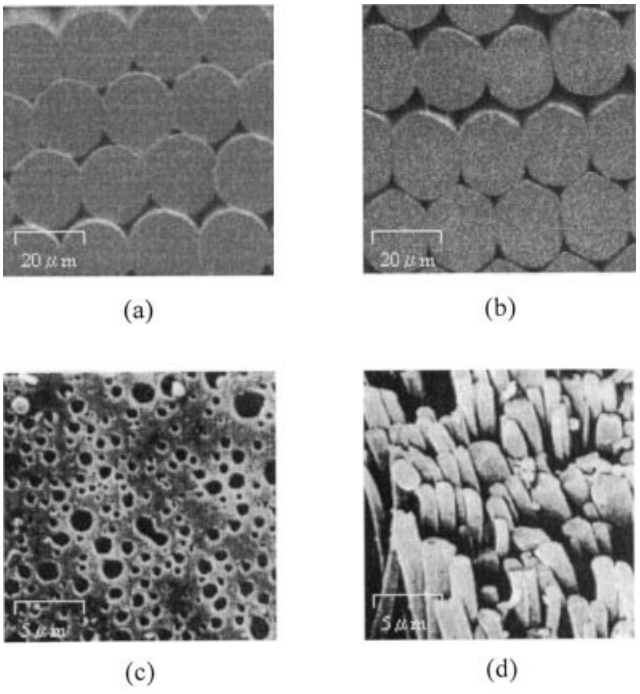

Figure 7 Morphologies of PA 6, m-iPP, and PA 6/m-iPP conjugated filaments: (a) 100/0 PA 6/m-iPP, (b) 0/100 PA 6/m-iPP, and (c) 50/50 PA 6/m-iPP after a formic acid treatment and (d) 50/50 PA 6/m-iPP after a xylene treatment.

terfacial interactions between PA 6 and m-iPP indicated poor mechanical properties. The tendency agreed with the flow behavior, and the 50/50 PA 6/m-iPP blend displayed a minimum tenacity value. Figure 9 displays the relationship between the densities and blend ratios of the PA 6/m-iPP conjugated filaments. For all PA 6/m-iPP conjugated filaments, the experimental densities agreed fairly well with the calculated values. This indicated that PA 6 and m-iPP formed an immiscible system. The experimental results for the densities were consistent with the thermal behavior, flow behavior, crystallinity, mechanical properties, and morphologies from SEM pictures of the PA 6/m-iPP conjugated filaments.

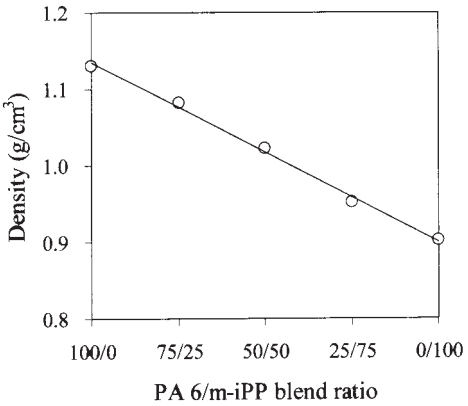

Figure 9 Relationship between the density and blend ratio of PA 6/m-iPP conjugated filaments.

CONCLUSIONS

The PA 6 polymer possesses amide-functional groups (—NHCO— groups). Furthermore, the m-iPP polymer does not possess any functional groups. The interfacial adhesion plays a critical role for PA 6/m-iPP conjugated filaments. The flow behavior of PA 6/m-iPP polyblended polymers exhibited NDBs. A 50/50 PA 6/m-iPP blend showed a lower value of the melt viscosity than that predicted by the additivity rule. The rheological results indicated poor interfacial adhesion between the PA 6 and m-iPP polymers. The experimental results from DSC indicated that the PA 6 and m-iPP molecules easily formed individual domains. The tenacities of the PA 6/m-iPP conjugated filaments declined initially and then increased with the proportion of m-iPP. Obviously, the 50/50 PA 6/m-iPP blend displayed a minimum value. The experimental crystallinities and densities agreed fairly well with the calculated values. This indicated that PA 6 and m-iPP formed an immiscible system. The morphological results could imply that PA 6 and m-iPP could be divided into two parts. From the flow behavior, thermal behavior, crystallinity, mechanical properties, density measurements, and morphological observations of the conjugated filaments. The PA 6/m-iPP polymers were proved to be an immiscible system.

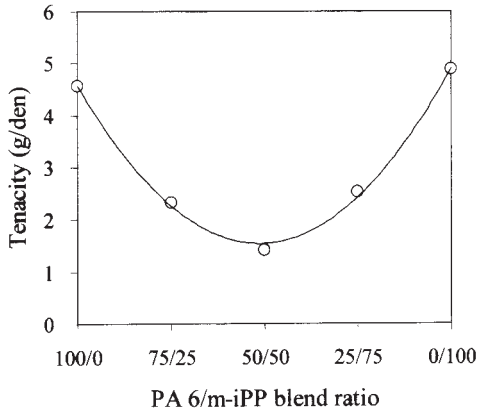

Figure 8 Relationship between the tenacity and blend ratio of PA 6/m-iPP conjugated filaments.

References

1. Vinogradov, G. V.; Yarlykov, B. V.; Tsebrenko, M. V.; Yudin, A. V.; Ablazova, T. I. Polymer 1975, 16, 609.
2. Ablazova, T. I.; Tsebrenko, M. V.; Yudin, A. V.; Vinogradov, G. V.; Yarlykov, B. V. J Appl Polym Sci 1975, 19, 1781.
3. White, J. L.; Plochoki, A. P.; Tanaka, H. Polym Eng Rev 1981, 1, 217.
4. Barlow, J. W.; Paul, D. R. Polym Eng Sci 1981, 21, 985.
5. Dimov, K.; Savov, M.; Georgiev, J. Angew Makromol Chem 1980, 84, 119.
6. Dimov, K.; Savov, M. Vysokomol Soedin A 1980, 22, 65.
7. Hsiao, K.; Shu, Y. C.; Tsen, W. C. J Polym Res 2003, 10, 161.
8. Hsiao, K.; Tsen, W. C.; Shu, Y. C. J Appl Polym Sci 2004, 91, 1710.
9. Evetative, M.; Fakirov, S. Polym Networks Blends 1994, 4, 25.
10. Serpe, G.; Jarrin, J.; Dawans, F. Polym Eng Sci 1990, 30, 553.
11. Li, F.; Chen, Y.; Zhu, W.; Zhang, X.; Xu, M. Polym 1998, 39, 6929.
12. Willis, J. M.; Favis, B. D. Polym Eng Sci 1988, 28, 1416.
13. Willis, J. M.; Caldas, V.; Favis, B. D. J Mater Sci 1991, 26, 4742.
14. Tsen, W. C.; Shu, Y. C.; Hsiao, K.; Jen, Z. F. J Polym Res 2004, 11, 189.
15. Hsiao, K.; Jen, Z. F.; Tsen, W. C.; Shu, Y. C. J Appl Polym Sci 2005, 97, 1220.
16. Steinkamp, R. A.; Grail, T. J. U.S. Pat. 3,862,265 (1975).
17. Koyama, K.; Suryadevara, J.; Spuriell, J. E. J Appl Polym Sci 1986, 31, 2203.
18. Kunugi, T.; Suzuki, A.; Hashimoto, M. J Appl Polym Sci 1981, 26, 1951.
19. Hsiao, K. J.; Jen, Z. F.; Lu, C. L. M. J Appl Polym Sci 2002, 86, 3601.
20. Hsiao, K. J.; Jen, Z. F.; Yang, J. C.; Chen, L. T. J Polym Res 2002, 9, 53.
21. Wunderlich, B. Therm Anal 1990, 424.
22. Godshall, D.; White, C.; Wilks, G. L. J Appl Polym Sci 2001, 80, 130.
23. Utracki, L. A. Polym Eng Sci 1983, 23, 602.
24. Han, C. D.; Kim, Y. W. J Appl Polym Sci 1975, 19, 2831.
25. Kasajima, M. Bull Colloid Eng Hosei University 1979, 15, 1.
26. Shin, C. K. Polym Eng Sci 1976, 16, 742.
27. Patterson, D. D. Polym Eng Sci 1982, 22, 64.
28. Kohan, M. I. Nylon Plast 1973, 278.
29. Eric, B. B.; Joseph, E. S. J Appl Polym Sci 2001, 81, 229.
30. Modoki, M.; Kawaguchi, T. J Polym Sci Polym Phys Ed 1977, 15, 1067.
31. Varga, J. J Mater Sci 1992, 27, 2557.
32. Eric, B. B.; Joseph, E. S. J Appl Polym Sci 2001, 82, 3237.